

THE MOLECULAR DYNAMICS OF OPTICALLY ACTIVE LIQUIDS: THE BROMOCHLOROFLUOROMETHANES

MYRON W. EVANS

Chemistry Department, University College of Wales, Aberystwyth, Dyfed SY23 1NE  
(Gt. Britain)

(Received 19 May 1983)

ABSTRACT

The molecular dynamics of R and S bromochlorofluoromethane and its racemic mixture have been investigated in the liquid state with computer simulation. There are intrinsic differences in the molecular dynamics of the two enantiomers which can be quantified clearly in the moving frame of the principal moments of inertia. When the two liquid enantiomers are mixed in equimolar proportion these differences result in a racemic modification of the molecular dynamical properties of the mixture as compared with those of either component. The racemic modification is measurable in a series of laboratory frame auto-correlation functions and is attributed to the statistical correlation between the centre of mass linear velocity,  $v$  of a molecule and its own angular momentum,  $J$ , at subsequent instances along the overall dynamical trajectory of that molecule.

INTRODUCTION

The science of the optically active molecule's rototranslation in the gaseous liquid and solid states is full of interest and in its infancy. It is therefore rewarding to look in detail at one of the smallest of the available optically active molecules, bromochlorofluoromethane, using computer simulation to suggest a range of observable liquid state phenomena in the laboratory frame of reference. Two of the most interesting of these are vibrational optical activity in the infra-red and Raman discovered [1-6] by Atkins, Barron, Buckingham and Bogaard and observed recently in the gas, liquid and solid states of simple, optically active molecules.

Due to the careful work of Burow et al. [7-9] and of Jacob [10], the structural characteristics of the  $\text{CHBrClF}$  molecule are known. The principal

cartesian coordinates are available in the literature [9] and the principal moments of inertia may be calculated therefrom as  $I_A = 131.34 \times 10^{-40} \text{ gm cm}^2$ ;  $I_B = 419.17 \times 10^{-40} \text{ gm cm}^2$ ;  $I_C = 532.61 \times 10^{-40} \text{ gm cm}^2$ . A calculation of this kind for  $C_1$  chiral symmetry is not trivial, requiring an iterative minimisation algorithm. The principal cartesian frame of the R and S enantiomers is shown in fig. (1). This coincides neither with the principal polarisability frame nor

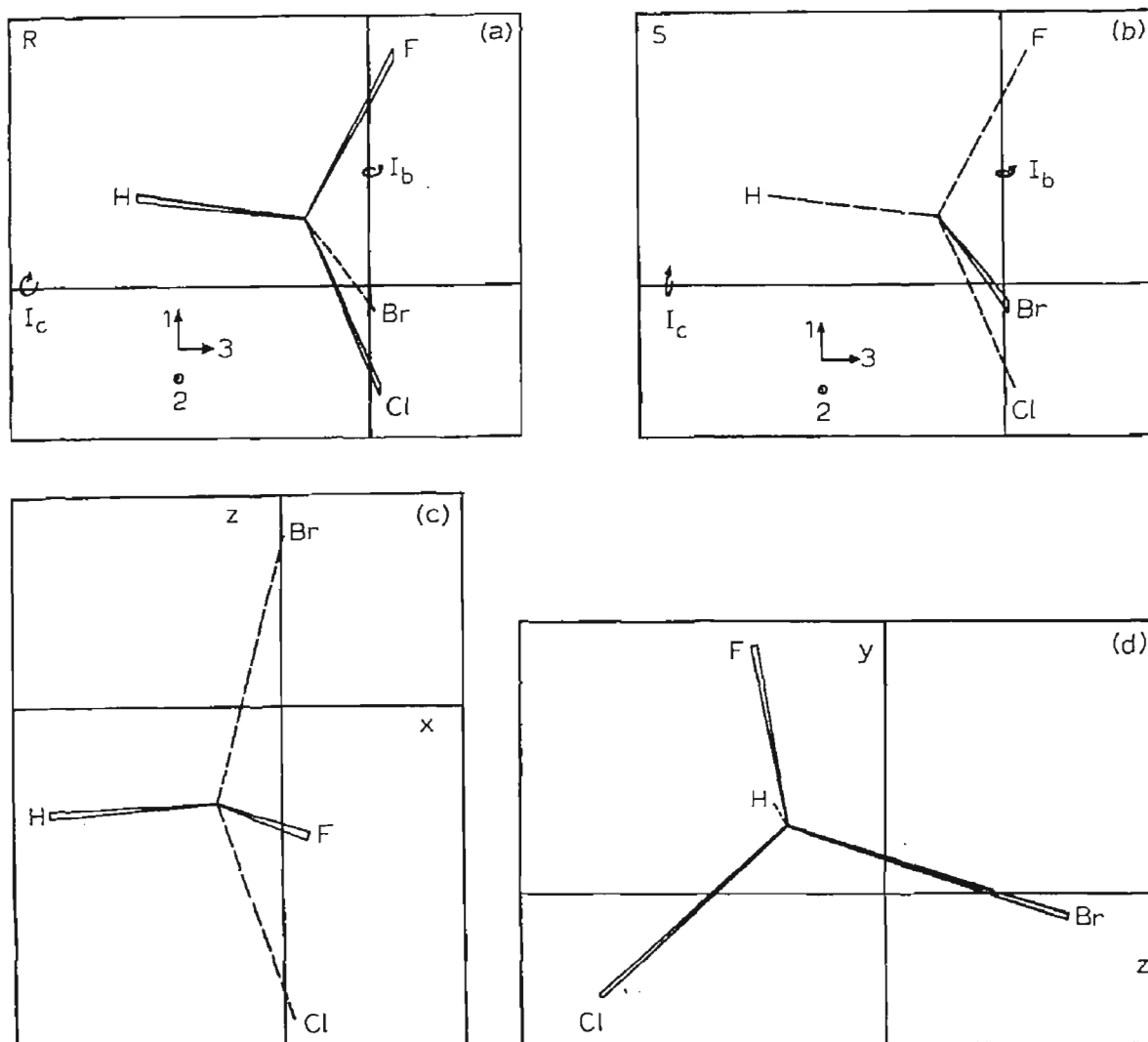


Fig. 1. Projections of CHBrClF in the principal moment of inertia frame.

(a) R enantiomer, inset: the frame of  $\underline{e}_1$ ,  $\underline{e}_2$  and  $\underline{e}_3$ .

(b) As for (a), S enantiomer.

(c) and (d) Projections in mutually orthogonal planes. These illustrations were drawn using the principal cartesian coordinates of ref. (9).

with that of the symmetry-obscured friction tensor of the phenomenological theory of Brownian motion [11].

Prasad and Burow [9] have reported the Raman and infra-red spectra of HCB<sub>2</sub>ClF in the gaseous, liquid and solid states. Their paper prepares the way for the future observation of vibrational optical activity for which HCB<sub>2</sub>ClF is a model. There are nine vibrational fundamentals which appear in the gas phase at  $\nu_1 = 3025.7 \text{ cm}^{-1}$ ;  $\nu_2 = 1310.9 \text{ cm}^{-1}$ ;  $\nu_3 = 1205.0 \text{ cm}^{-1}$ ;  $\nu_4 = 1078.3 \text{ cm}^{-1}$ ;  $\nu_5 = 787.8 \text{ cm}^{-1}$ ;  $\nu_6 = 663.8 \text{ cm}^{-1}$ ;  $\nu_7 = 426.7 \text{ cm}^{-1}$ ;  $\nu_8 = 314.5 \text{ cm}^{-1}$  and  $\nu_9 = 225.7 \text{ cm}^{-1}$ . All are infra-red and Raman active since there is no symmetry. These data are for the racemic mixture, because the enantiomers have not been separated yet in the laboratory. The simple, pentatomic, vibrational spectra are complicated by a number of combination and difference bands, all allowed for C<sub>1</sub> (chiral) symmetry. Some of these are enhanced intensely by Fermi resonance [12]. There are considerable shifts between the spectra in the gaseous, liquid and solid states. In the far infra-red gas phase spectrum for a C<sub>1</sub> symmetry where none of the bonds coincides with an inertial axis, hybrids of A, B and C type band contours are expected underneath the observed envelopes. The solid state spectra are difficult to interpret [9]. The band-widths decrease from the liquid state, but splittings are observable in modes which involve the appreciable motion of the F atom. Prasad and Burow [9] mention in this context the possible existence of RR, RS and SS enantiomer pairs in their solid state samples. From the group theory of the Raman effect all the vibrations in C<sub>1</sub> symmetry are polarised, and neither the isotropic nor anisotropic part of the polarizability tensor is zero. No local symmetry is possible and it is feasible in consequence to measure the depolarisation ratios of modes which involve the asymmetric centre. It is one of the aims of this paper to show that this allows us to look directly at the statistical correlation between the translation of the centre of mass in HCB<sub>2</sub>ClF and its own rotational motion about this centre of mass.

The obscure internal field corrections in the literature on Raman spectroscopy do not work [9] on going from gas to liquid in HCB<sub>2</sub>ClF. Prasad and Burow conclude therefore that "substantial inter-molecular interactions prevail in the liquid". These authors mention that the medium effects in the liquid depend on the vibrational fundamental under observation, i.e. are different for different fundamentals. Again, these data refer to the racemic mixture and may differ in nature for either pure enantiomer. Rototranslational inter-molecular effects are studied in detail later in this paper using computer simulation of the liquid state of HCB<sub>2</sub>ClF. The results of Prasad and Burow [9] imply that vibration/rotation correlation is present in the liquid, our computer simulation clearly

details the nature of the correlation between molecular rotation and translation by comparing the spectrum of an enantiomer with that of the racemic mixture.

Some calculations of the vibrational circular dichroism [1-6] of HCB<sub>2</sub>ClF are available [13-16] in the literature from several groups. Prasad and Nafie [13] point out that the different response to left and right circularly polarised light in this effect, and in the analogous Raman effect (Raman optical activity [6]) can be used to give unique stereochemical information for chiral molecules in the random phase. Their calculation uses the atom-dipole formalism, each atom being associated with an isotropic polarisability. These are then coupled dynamically via a dipole interaction function causing the atomic polarisabilities to become anisotropic. This method was also used by Applequist [14] who expressed optical rotation in HCB<sub>2</sub>ClF in terms of a set of relay tensors, which describe the manner in which the external field acting at one unit of the molecule induces a dipole moment in another unit. The rotation of polarised light is expressed in terms of electric and magnetic moments associated with certain sets of normal modes. Recently Sundberg [15] has extended these calculations to involve higher order terms in the unit polarisabilities, and thereby non-linear response to incoming polarised fields of radiation for frequencies well away from any molecular resonance.

When the elements of the diagonalised atom polarisability tensors are equal, the models [12] used in these papers reduce to point-charges located at the atomic sites. The work of Diem et al. [7,8] and Nafie et al. [16] provides us in this context with the following optimised values of three partial charges, which we use in this paper in our model of the pair potential for HCB<sub>2</sub>ClF:

$q_F = -0.22e$  ;  $q_{Cl} = -0.18e$  ;  $q_{Br} = -0.16e$  ;  $q_C = 0.335e$  ;  $q_H = 0.225e$  ;  
where  $e$  is the electronic charge.

It is important to note that both vibrational circular dichroism and Raman optical activity depend on

- 1) using circularly polarised radiation probes;
- ii) having available pure R and S enantiomers.

These effects are intra-molecular in origin but may be affected by the surrounding medium, e.g. may lead to different spectra in the gas and liquid. In contrast, we have observed [17-19] by computer simulation an intrinsic difference in the nature of enantiomer R and S of any chiral molecule in the liquid state. This reveals itself in the different nature of the statistical correlation between rotation and translation already mentioned. This difference is independent of the nature of any radiation field which may be used to look at the R and S enantiomer, and leads to physical and spectral differences between enantiomer and racemic mixture. These differences are well-known, are sometimes large

and sometimes small. There is no reason why they should not persist in the solid and compressed gaseous states of matter. They should be especially persistent in the supercooled liquid state where rotation/translation correlation is pronounced [20]. Using simple empirical arguments based on the differences in molecular configuration of any pair of enantiomers R and S, Evans [21] has suggested that they are maximised when the centre of mass displacements involved in creating R from S by switching any two atoms are maximised. This hypothesis leads to certain chiral geometries, such as that of HCB<sub>2</sub>ClF, where large spectral differences between enantiomer and racemic mixture should be observable in the laboratory frame, and large intrinsic differences between R and S in the relevant moving frame of reference. It might be oversimplified, but at the same time an useful aid to understanding, to state that any two of the four atoms attached to carbon in HCB<sub>2</sub>ClF differ markedly in atomic weight, and that this "offset" mass distribution leads to a large intrinsic difference between the rototranslational molecular dynamics of the R and S liquids. These differences are normally visible only in the moving frame [22] of reference of the computer, for convenience that of the principal moments of inertia, and remain hidden in the laboratory frame except to techniques such as vibrational circular dichroism and Raman optical activity, which would report them indirectly as media effects. Mixing enantiomers R and S in equimolar proportions produces a different overall symmetry in the statistical correlation between molecular rotation and translation from that in either enantiomer, and this difference becomes visible in the laboratory frame in a direct and straightforward manner by comparing mixture with component.

The HCB<sub>2</sub>ClF molecules suited to a more detailed study of rototranslational correlation than we have reported to date because of the papers reviewed already and also because its thermodynamical properties have been collated by Kudchadker et al. [23,24]. These authors have analysed the available data on HCB<sub>2</sub>ClF from the boiling point to the critical point with the Antoine and Wagner equations. Molecular parameters, fundamental frequencies, enthalpies of formation etc. have been evaluated critically by these authors and recommended values selected for  $C_p^0$ ;  $S^0$ ;  $(H^0 - H_0^0)$ ;  $-(G^0 - H_0^0)/T$ ;  $\Delta H_j$ ;  $\Delta G_j$  and  $\log K_f$  from 0 to 1500K at 1bar using the rigid rotor harmonic oscillator approximation. These data help to construct a qualitatively acceptable 5 x 5 site-site pair potential for our computer simulation, using Lennard-Jones parameters and the partial charges mentioned already.

Finally, we refer to the calculation of <sup>13</sup>C NMR chemical shifts in HCB<sub>2</sub>ClF carried out by Somayajulu et al. [25] using methods akin to those of Applequist [26],

and Sundberg [15], and an interesting paper by Bonchev et al. [26] on the information content of chiral structures such as those of HCB<sub>2</sub>ClF. According to Bonchev et al. the information available generally from molecular symmetry data exceeds that from topological and chemical compound sources. These authors have studied the influence of the degree of symmetry on systems containing an equal number of atoms. Their paper supports our suggestion that the lower the symmetry of simple molecules, the greater the information available and observable in terms of molecular physical properties. The computer now allows us to deal with the technical difficulties of asymmetric-top dynamics, and circumvent the formidable problems posed even by the simplest phenomenological theory [11] of molecular diffusion in the low symmetry limit.

#### COMPUTER SIMULATION METHODS

These have been standardized by the S.E.R.C. CCP5 group and we concentrate here on the implementation of the algorithm TETRAH by Ferrario and Evans [27,28]. The periodic boundary conditions and minimum image conventions of the molecular dynamics simulation method are implemented with an improved numerical method of solving the equations of motion. The intermolecular pair potential is modelled with site-site terms based on Lennard-Jones and partial charge interactions. The parameters used in this computation are given in table 1. In this preliminary study no attempt was made to optimise the Lennard-Jones parameters and the output thermodynamic data are summarised in table 2 for the two enantiomers and the racemic mixture. After a stabilisation (equilibration) period of about 3500 time steps the dynamical data from the simulation were stored on disk and running-time averaging used to construct correlation functions. In the racemic mixture 54 molecules were of type S and 54 of type R. The input state point was 273K, 1bar.

#### RESULTS AND DISCUSSION

##### CROSS-CORRELATIONS IN THE MOVING-FRAME OF REFERENCE

If we denote the elements of the moving frame cross-correlation matrix  $\langle \underline{v}(t) \underline{J}^T(0) \rangle_m$  by (1,1) etc. to (3,3), then a total of nine normalised cross-correlation functions can be extracted from the data generated in the computer simulation. For example, the (1,2) element in normalised form is:

$$(1,2) \equiv \frac{\langle v_1(t) J_2(0) \rangle_m}{\langle v_1^2 \rangle_m^{1/2} \langle J_2^2 \rangle_m^{1/2}} \quad (1)$$

In CHBrClF the off-diagonal elements of this matrix exist for  $t > 0$  but the diagonal elements vanish by symmetry for all  $t$ . The off-diagonal elements provide a detailed description of the statistical correlation between a molecule's

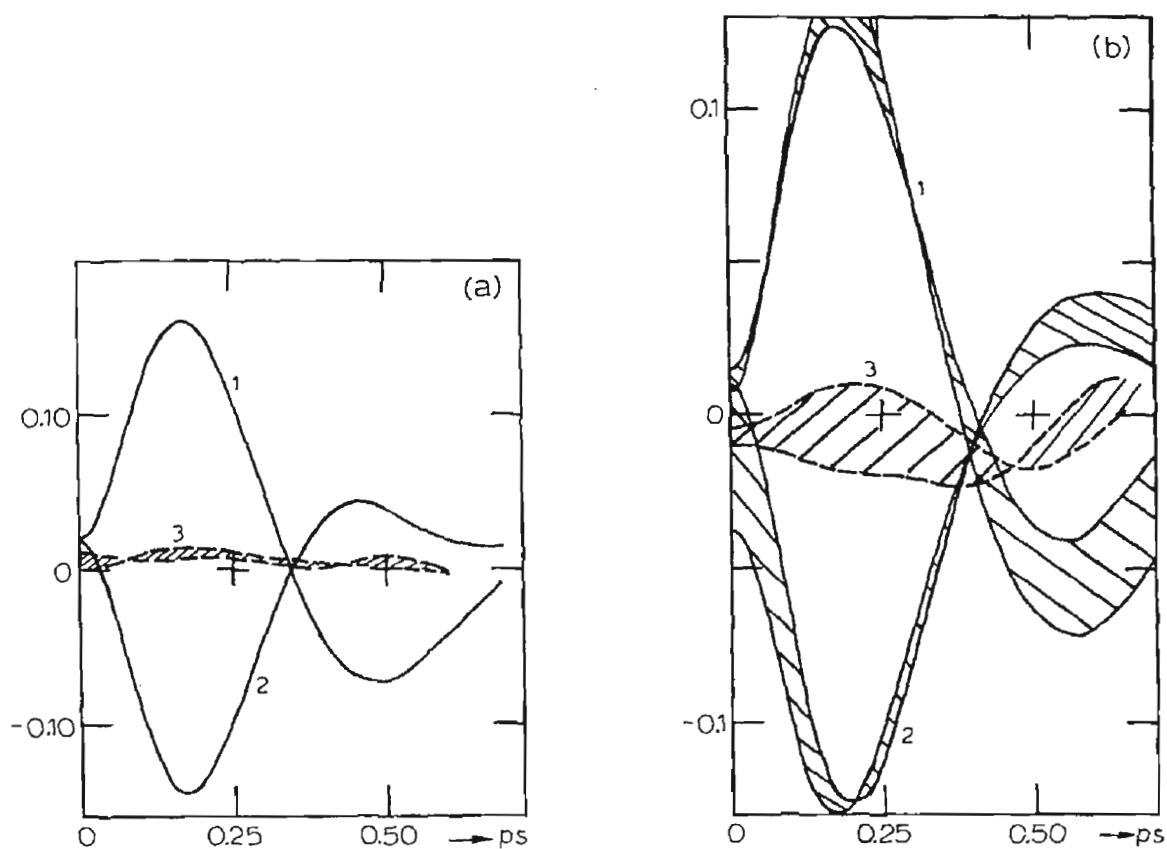


Fig. 2. Moving frame elements of  $\langle \underline{v}(t) J^T(0) \rangle_m$ , normalised as in the text.

- (a) (1) (3,1) element for the S enantiomer.  
 (2) (3,1) element for the R enantiomer.  
 (3) (3,1) element for the racemic mixture.

- (b) (1) (1,3) element for the R enantiomer.  
 (2) (1,3) element for the S enantiomer.  
 (3) (1,3) element for the racemic mixture.

} Hatched area  
 represents  
 noise level

Abcissa: time/ps.

centre of mass translation and its own rotation, measured here through the angular momentum  $\underline{J}$ . Correlations exemplified by eqn. (1) are not considered in the phenomenological theory of molecular diffusion [11] but are nevertheless of basic importance, as illustrated for the R and S enantiomers and racemic mixture of  $\text{CHBrClF}$  in figs (2) to (4).

These figures show quite clearly the intrinsic difference between the properties of R and S enantiomer pairs. For example, (3,1) in the S enantiomer is positive (fig. 2(a)) and negative in the R enantiomer. In the racemic mixture (3,1) is very small, and buried in the "noise" generated by our relatively low-power computer (CDC 7600). (The noise level can be judged by the fact that all (3,1) elements should vanish at  $t = 0$ .) Longer runs on the Cray system would provide a much better "signal to noise ratio".

In fig. 1(b) we illustrate that (1,3) is positive for the R enantiomer, negative for the S and is unmeasurably small in the racemic mixture.

In contrast, (1,2) is positive in all three cases and (2,1) negative (fig. (3)). It seems that these elements are the same, within the "noise" in both enantiomers, but decreased in magnitude and shifted slightly along the time axis in the racemic mixture. Note that (1,2) is not the mirror image of (2,1). In the enantiomers, the magnitude of the elements in figs (2) and (3) decrease as:

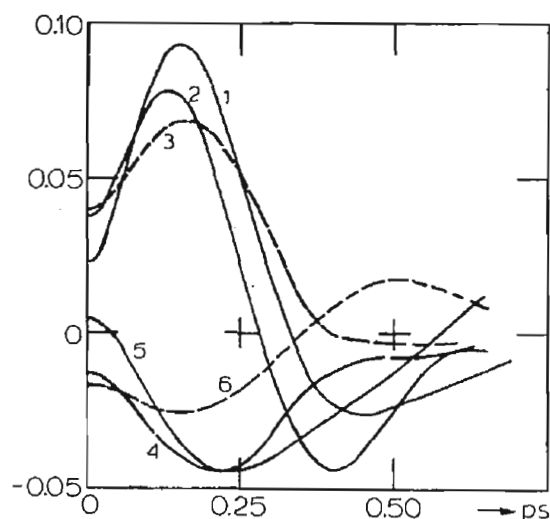


Fig. 3. (1) (1,2) element, S enantiomer. (2) (1,2) element, R enantiomer.  
 (3) (1,2) element, racemic mixture. (4) (2,1) element, S enantiomer.  
 (5) (2,1) element, R enantiomer. (6) (2,1) element, racemic mixture.  
 Abscissa: time/ps.



$|(3,1)| > |(1,3)| > |(1,2)| > |(2,1)|$ , where  $|(\ )|$  denotes "the maximum value of". In the racemic mixture  $|(1,2)| > |(2,1)| > |(3,1)| = |(1,3)| = 0$ .

In fig. (4), we illustrate the (2,3) and (3,2) elements, which are the smallest in magnitude and only just measurable above the "noise". The pattern is different from figs. (2) and (3). The (2,3) and (3,2) elements are not mirror images but this time it seems that (2,3) for the racemic mixture is intermediate in magnitude between the smaller (2,3)(S) and larger (2,3)(R). There is also a regular shift along the time axis from S through RS to R (fig. 4(a)). However the noise level is almost at that of the signal. Finally, in fig. 4(b), the smallest elements (3,2) provide us with another different pattern of behaviour, the racemic mixture this time being slightly negative and the two enantiomer elements perhaps very slightly positive above the noise.

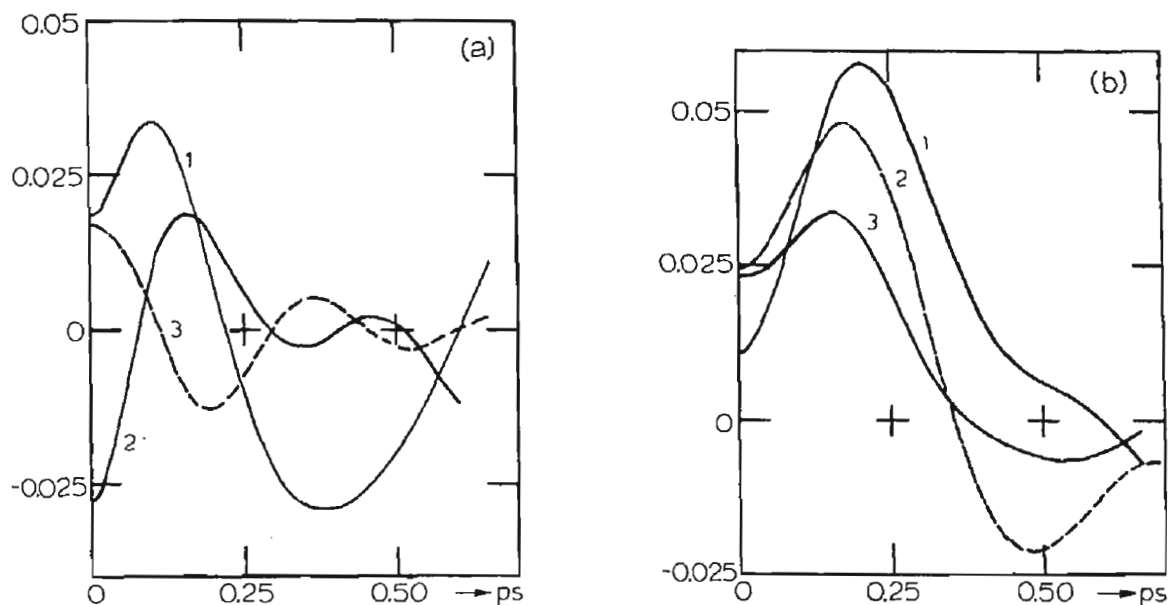


Fig. 4.

- (a) (1) (2,3) element for the R enantiomer.  
 (2) (2,3) element for the racemic mixture.  
 (3) (2,3) element for the S enantiomer.  
 (b) (1) (3,2) element for the R enantiomer.  
 (2) (3,2) element for the S enantiomer.  
 (3) (3,2) element for the racemic mixture.

Abcissa: time/ps.

TABLE 1  
Structural and Potential Data used for HBrClF

Atom	Principal Cartesian Coordinates <sup>a</sup> /Å				Lennard-Jones Parameters <sup>b</sup>		Partial Charges <sup>c</sup> / e
	x( <u>e</u> <sub>3</sub> )	y( <u>e</u> <sub>1</sub> )	z( <u>e</u> <sub>2</sub> ) (R)	z( <u>e</u> <sub>2</sub> ) (S)	ε/k/K	σ/Å	
Br	0.0216	-0.1613	-1.1283	1.1283	218.0	3.9	-0.16
C	-0.4362	0.4531	0.6393	-0.6393	35.8	3.4	0.335
H	-1.5565	0.5928	0.7215	-0.7215	10.0	2.8	0.225
Cl	0.0581	-0.6952	1.8681	-1.8681	158.0	3.6	-0.18
F	0.1603	1.6403	0.8651	-0.8561	54.9	2.7	-0.22

(a) P. L. Prasad and D. F. Burow, J. Am. Chem. Soc., 1979, 101 806.

(b) E. L. Eliel, N. L. Allinger, S. J. Angyal and G. A. Morrison, "Conformational Analysis", Wiley, N.Y., (1965).

(c) from L. A. Nafie, P. L. Polavarapu and M. Diem, J. Chem. Phys., 1980, 73, 3530.

$$I_A = 131.34 \times 10^{-40} \text{ gm cm}^2$$

$$I_B = 419.17 \times 10^{-40} \text{ gm cm}^2$$

$$I_C = 532.61 \times 10^{-40} \text{ gm cm}^2$$

Therefore there is a rich variety of detail in this single moving frame correlation matrix alone. This is sensitive to details of the inter-molecular potential and the thermodynamic conditions of pressure, temperature and volume under which the run is made. This type of moving frame matrix is the key to that which becomes visible to the observer in the laboratory frame of reference. In other words, what appears to us as a liquid state spectrum is the result of a large number of molecular statistical correlations such as those sketched out in figs (2) to (4) (using a semi-quantitative model for the true intermolecular potential energy surface in CHBrClF).

#### LABORATORY FRAME OF REFERENCE - THE RACEMIC MODIFICATION

The racemic modification of physical properties was discovered by Pasteur in the tartaric acids and exemplified by the drop in melting point between R or S enantiomer and racemic mixture. In the lactic acids this is 35K and therefore easily measurable. In other cases the racemic modification of physical properties

TABLE 2

Input = 273K

Thermodynamic Output After 4 Cycles (4000 time steps approx.).

<u>S Enantiomer</u>	<u>R Enantiomer</u>
Mean Pressure = 527 bar	Mean Pressure = 679.7 bar
$\langle p^2 \rangle = 3.64 \times 10^5$ bar	$\langle p^2 \rangle = 5.17 \times 10^5$ bar
Total energy = $-31.6 \text{ kJmole}^{-1}$	Total Energy = $-31.2 \text{ kJmole}^{-1}$
$\langle T_{\text{tr.}} \rangle = 277$ K	$\langle T_{\text{tr.}} \rangle = 275.2$ K
$\langle T_{\text{rot}} \rangle = 274$ K	$\langle T_{\text{rot}} \rangle = 270.5$ K
$\langle \text{Pot. En} \rangle = -38.5 \text{ kJmole}^{-1}$	$\langle \text{Pot. En} \rangle = -38.0 \text{ kJmole}^{-1}$
$\langle \text{Virial} \rangle = -5.0 \text{ kJmole}^{-1}$	$\langle \text{Virial} \rangle = -8.6 \text{ kJmole}^{-1}$

Racemic Mixture

Mean Pressure = 919.4 bar
$\langle p^2 \rangle = 9.50 \times 10^5$ bar
Total Energy = $-30.8 \text{ kJmole}^{-1}$
$\langle T_{\text{tr.}} \rangle = 273.0$ K
$\langle T_{\text{rot}} \rangle = 275.3$ K
$\langle \text{Pot. Energy} \rangle = -37.7 \text{ kJmole}^{-1}$
$\langle \text{Virial} \rangle = -14.0 \text{ kJmole}^{-1}$

Bromochlorofluoromethane

such as boiling point, density, refractive index and so on is small but measurable. There are no differences between the physical properties of two (R and S) enantiomers (except in their response to a symmetry breaking variable such as a circularly polarised electromagnetic radiation field).

We have to square this information with that in figs. (2) to (4). where pronounced differences in the physical (i.e. dynamical) properties of enantiomers and racemic mixture become visible. The only possible way of doing this is to conclude that it is the overall symmetry of  $\langle \underline{v}(t) \underline{J}^T(0) \rangle_m$  which matters in the laboratory frame of reference. The symmetry of this moving frame matrix is given below for the R and S enantiomers and racemic modification.

0 + +	0 + -	0 + 0
- 0 +	- 0 +	- 0 +
- $\delta$ + 0	+ $\delta$ + 0	0 $\delta$ - 0
(R)	(S)	(RS)

The matrix in both enantiomers has a single diagonal of zero elements, whereas both diagonals in the racemic mixture are made up of zero elements.

The effect of this in the laboratory frame of reference is illustrated in figs. (5) to (10) using a range of autocorrelation functions of the following vectors.

- i)  $\underline{v}$  and  $\underline{J}$  in their usual laboratory frame definition;
- ii) the laboratory frame molecular angular velocity,  $\underline{\omega}$ ;
- iii) the force and torque vectors  $\underline{F}$  and  $\underline{T}_q$  measuring the resultant force and torque on the CHBrClF molecule;
- iv) the orientational unit vectors  $\underline{l}_1$ ,  $\underline{l}_2$  and  $\underline{l}_3$  and their time derivatives  $\dot{\underline{l}}_1$ ,  $\dot{\underline{l}}_2$  and  $\dot{\underline{l}}_3$ .

The laboratory frame autocorrelation functions should be the same in all cases for the R and S enantiomers and this provides us with a check on the "noise level" in the laboratory frame, and on any artifact coming from the use of periodic boundary conditions, minimum image convention, virial corrections, etc. of the theoretical method of computer simulation.

In fig. (5) we illustrate the orientational autocorrelation functions  $\langle \underline{l}_1(t) \cdot \underline{l}_1(0) \rangle$ ,  $\langle \underline{l}_2(t) \cdot \underline{l}_2(0) \rangle$  and  $\langle \underline{l}_3(t) \cdot \underline{l}_3(0) \rangle$ . The results in all three cases for the R and S enantiomers are almost identical on the scale of this figure, but those for the racemic mixture are clearly different. We make the hypothesis that the origin of this difference lies in the nature of cross-correlations such as those illustrated in figs. (2) to (4). The molecular dynamical ensemble can be described with Newton's equations, which involve two basic variables,  $\underline{v}$  and  $\underline{J}$ . Therefore the racemic modification of molecular dynamical properties can be traced to the statistical correlation between these two vectors, representing molecular centre of mass translation and molecular angular momentum. In classical mechanics all else follows from this.

The whole of the phenomenological theory of molecular diffusion rests on the assumption that multi-body dynamics are too complicated to be tractable with Newton's equations. As a consequence, the class of equations exemplified by those of Langevin and Fokker and Planck, and, more recently, Kramers, have been used [11] to describe, for example, spectral observables in terms of phenomenological coefficients. The best-known of these is the Debye relaxation time,  $\tau_D$ . These manage to describe what is observable, but cannot provide us with the information illustrated in figs. (2) to (4). In practice, the phenomenological theory runs into difficulties and complexity as soon as one departs from the simple and clear exercise carried out by Debye in 1912-1913.

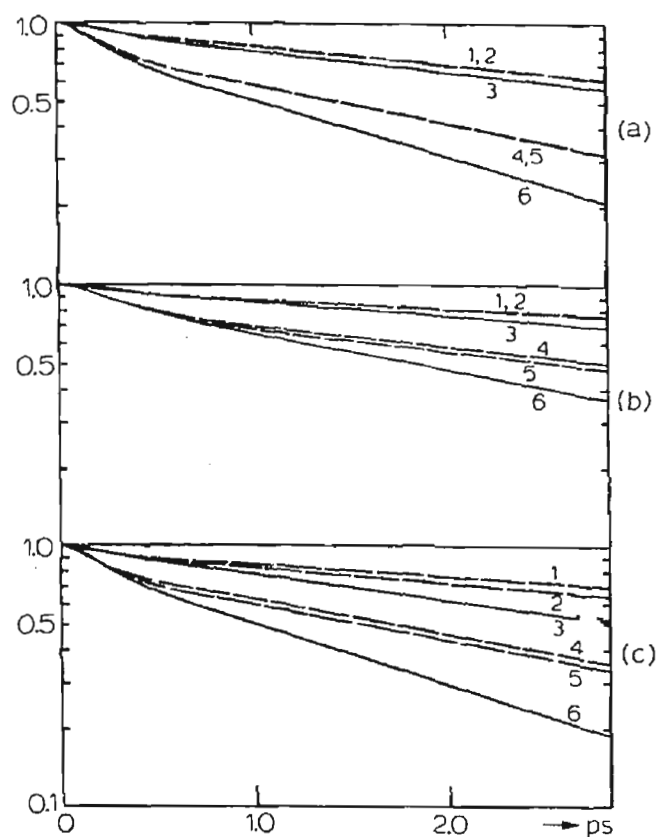


Fig. 5. Semi-logarithmic plots of the orientational autocorrelation functions in the laboratory frame of reference for the two enantiomers and racemic mixture. (a) of  $\underline{l}_1$ ; (b)  $\underline{l}_2$ ; (c)  $\underline{l}_3$ . In each case: (1)  $P_1, S$ ; (2)  $P_1, R$ ; (3)  $P_1, RS$ ; (4)  $P_2, S$ ; (5)  $P_2, R$ ; (6)  $P_2, RS$ . The two enantiomers are hatched together for clarity.

Abscissa: time.ps.

It is significant that the phenomenological theory has never been used to attempt to describe, let alone explain, the racemic modification discovered by Pasteur some years ago prior to the Langevin equation. So far as we have not been able to find an example of an experimental investigation into the molecular dynamics of the racemic modification. The results exemplified in fig. (5) therefore provide both the experimentalist and analytical theoretician with original data. The problem to phenomenological theory can be put succinctly in terms of explaining why two liquids, with identical Debye relaxation times, dielectric, far infra-red spectra, etc., should produce different data when mixed in quimolar proportion. Grigolini et al. [28-31] have pointed out that the

answer lies in the development of non-linear equations reviewed recently by Suzuki [31] and Grigolini [29]. These methods are powerful and have been used to provide a more general base for quantum mechanics and field theory, i.e. are cross-disciplinary in application.

The enantiomers of CHBrClF have not yet been synthesized, but as mentioned in the introduction, spectral data and analysis are available on the racemic mixture.

In fig. (6) the pattern in fig. (5) is repeated for the rotational velocities  $\underline{\dot{l}}_1$ ,  $\underline{\dot{l}}_2$  and  $\underline{\dot{l}}_3$ . These laboratory frame autocorrelation functions can be related via a Fourier transformation to the far infra-red spectra of the enantiomers and racemic mixture. Both figs. (5) and (6) show that the rotational motion in CHBrClF is anisotropic in the laboratory frame. Analogously, all six roto-translational elements in figs. (2) to (4) are different, so that the overall motion of the molecule is also anisotropic. To generalise the phenomenological theory for this situation requires: i) three rotational friction coefficients, ii) three translational friction coefficients, iii) cross terms: a total of at least 27 coefficients assuming that all of these are diagonalisable in the same frame of reference. This frame is different from the principal moment of inertia frame and that of the molecular polarisability. This is the case even before attempting the inclusion of memory effects or non linear effects. There is clearly not enough spectral data to estimate these coefficients individually.

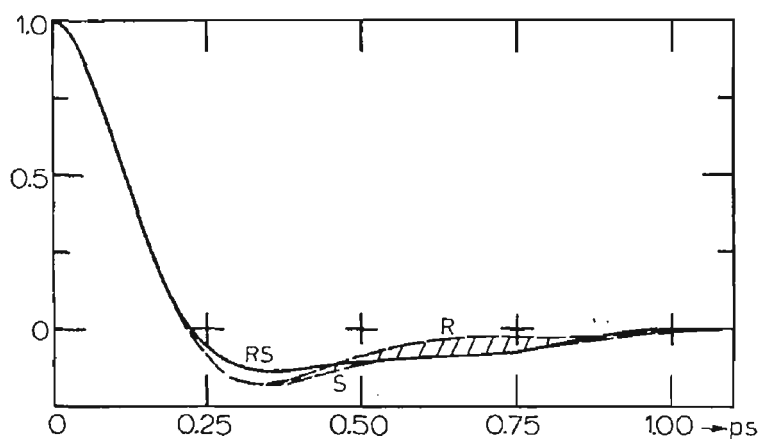


Fig. 6. Rotational velocity autocorrelation functions of  $\dot{l}_2$ ; (1) R enantiomer; (2) S enantiomer; (3) racemic mixture. The enantiomer functions are hatched together for clarity.

Abscissa: time/ps.

It is difficult to see how the phenomenological theory can attempt to describe the racemic modification without a fundamental development or simplification.

The first and second moment a.c.f.'s of angular velocity are illustrated in fig. (7), where the racemic modification moves the mixture function closer to the time origin, making it slightly more oscillatory. The second moment  $\langle \underline{\omega}(t) \cdot \underline{\omega}(t) \omega(0) \cdot \underline{\omega}(0) \rangle / \langle \omega^4 \rangle$  shows that the non-equilibrium statistical nature of the three systems are not Gaussian. The angular momentum a.c.f.'s behave very similarly to the angular velocity a.c.f.'s but the final levels attained by the

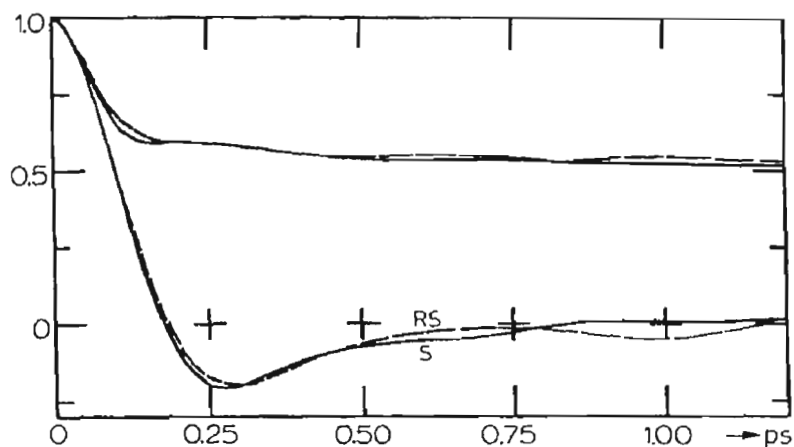


Fig. 7. Laboratory frame autocorrelation functions of molecular angular velocity. (1) R; (2) S; (3) RS; (4) R, second moment; (5) S, second moment; (6) RS, second moment.

Abscissa: time/ps.

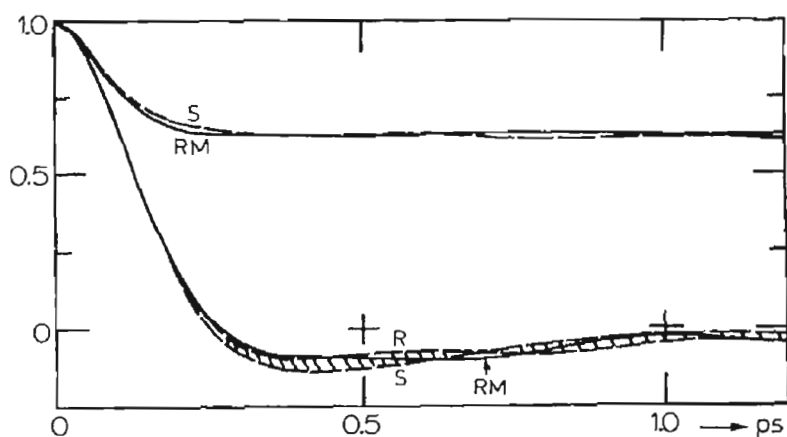


Fig. 8. As for fig. 7., centre of mass linear velocity.

second moments are not the same. Fig. (8) illustrates that the racemic modification in the centre of mass linear velocity a.c.f. is in the opposite sense to that of fig. (7), i.e. the centre of mass linear velocity a.c.f. of the racemic mixture is shifted to cut the time axis further from the origin, and is slightly less oscillatory. The long negative tails in these three a.c.f.'s ensure that their equivalent second moments do not reach the Gaussian level of 0.6 as  $t \rightarrow \infty$  until well into the time evolution from  $t = 0$ .

Finally, figs. (9) and (10) illustrate the racemic modification to the first and second moments of the torque and force a.c.f.'s, respectively, in the

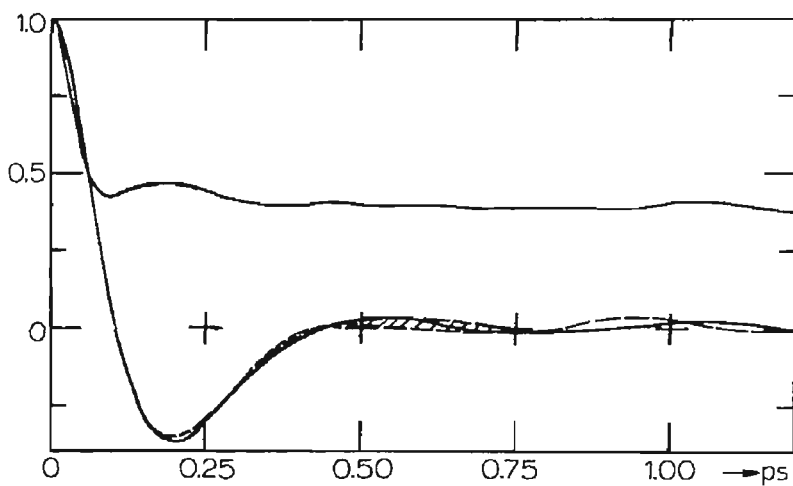


Fig. 9. As for fig. 7., torque.

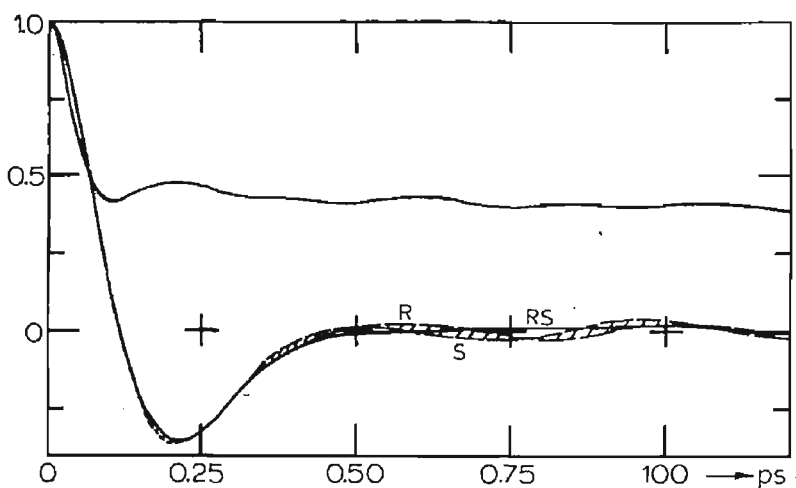


Fig. 10. As for fig. 7., force.



laboratory frame. In the functions the racemic modification is small, but real. The torque a.c.f. of the racemic mixture is slightly the less oscillatory and the force a.c.f. the more oscillatory.

The net effect of the pronounced moving frame differences of figs. (2) to (4) on the laboratory frame functions of figs. (5) to (10) therefore varies according to the vector considered. The most distinct laboratory frame effect is on the a.c.f.'s of  $\underline{l}_2$  and  $\underline{l}_3$ ,  $\underline{l}_2$  and  $\underline{l}_3$ , which means that the racemic modification should be observable with far infra-red and dielectric spectroscopy. We must wait for the synthesis of R and S CHBrClF for corroboration, but recent work [18] on naturally occurring enantiomers has indicated the existence of the far infra-red racemic modification in 3 methyl cyclohexanone, 3 methyl cyclopentanone and 2 aminobutanol. In the lactic acid systems at 293 K the modification is obvious because the racemic mixture is a liquid and each enantiomer a solid. This case is, however, complicated by hydrogen bonding. Molecular dynamics algorithms currently available for water or the alcohols could be adapted for use in the lactic acids (the 2-hydroxy propanoic acids).

#### SUMMARY OF CONCLUSIONS

- i) There is an intrinsic difference in the molecular dynamics of liquid R and S CHBrClF exemplified by the statistical correlation between molecular centre of mass linear velocity and angular momentum.
- ii) This is responsible for the racemic modification of molecular dynamical properties, observable in the laboratory frame.

#### ACKNOWLEDGEMENTS

The SERC and its CCP5 group are acknowledge for generous financial support and advice. The library of algorithms at SERC Daresbury is suitable for further work of this kind, and programmes will be despatched to interested workers free of charge. Librarian: Dr. W. Smith, SERC Daresbury, Nr. Warrington, WA4 4AD, U.K.

#### REFERENCES

- 1 P.W. Atkins and L.D. Barron, Mol. Phys., 16 (1969) 453.
- 2 L.D. Barron, J. Chem. Soc. (A) (1971) 2899.
- 3 A.D. Buckingham and L.D. Barron, Mol. Phys., 20 (1971) 1111.
- 4 L.D. Barron, M.P. Bogaard and A.D. Buckingham, Nature, 241 (1973) 113; J. Am. Chem. Soc., 95 (1973) 603.

- 5 A.D. Buckingham and L.D. Barron, J.C.S. Chem. Comm., (1973) 152; (1974) 1028.
- 6 L.D. Barron and A.D. Buckingham, Ann. Rev. Phys. Chem., 26 (1975) 381.
- 7 M. Diem and D.F. Burrow, J. Chem. Phys., 64 (1976) 5179;  
J. Phys. Chem., 81 (1977) 476.
- 8 M. Diem, L.A. Nafie and D.F. Burow, J. Mol. Spectrosc., 71 (1978) 446.
- 9 P.L. Prasad and D.F. Burow, J. Am. Chem. Soc., 101 (1979) 806.
- 10 E.J. Jacob, J. Mol. Struct., 52 (1979) 63.
- 11 M.W. Evans, G.J. Evans, W.T. Coffey and P. Grigolini, "Molecular Dynamics and Theory of Broad-Band Spectroscopy", Wiley/Interscience, N.Y., (1982) Chapter 2.
- 12 C. Marcott, T.R. Faulkner, A. Moscovitz and J. Overend, J. Am. Chem. Soc., 99 (1977) 8169.
- 13 P.L. Prasad and L.A. Nafie, J. Chem. Phys., 70 (1979) 5582.
- 14 J. Applequist, J. Chem. Phys., 58 (1973) 4251.
- 15 K.R. Sundberg, J. Chem. Phys., 68 (1978) 5271.
- 16 L.A. Nafie, P.L. Polavarapu and M. Diem, J. Chem. Phys., 73 (1980) 3530.
- 17 M.W. Evans, J. Chem. Soc., Chem. Comm., in press;  
Phys. Rev. Letters, in press;  
J.C.S. Faraday Trans. II, submitted.
- 18 M.W. Evans, J. Baran and G.J. Evans, J. Mol. Liquids, in press;  
J.C.S. Faraday II, submitted.
- 19 M.W. Evans and G.J. Evans, Nature, submitted.
- 20 M.W. Evans, computer simulation of ethyl chloride, J.C.S. Faraday II, in press.
- 21 M.W. Evans, J.C.S. Faraday II, *on pre.*
- 22 J.-P. Fyckaert, A. Bellemans and G. Ciccotti, Mol. Phys., 44 (1981) 979.
- 23 S.A. Kudchadker and A.P. Kudchadker, J. Phys. Chem., Ref. Data, 7 (1978) 1285.
- 24 A.P. Kudchadker, S.A. Kudchadker, R.P. Shukla and P.R. Patnaik, J. Phys. Chem., Ref. Data, 8 (1979) 499.
- 25 R.G. Somayajulu, J.R. Kennedy, T.M. Vickrey and B.J. Zwolinski, J. Magn. Res., 33 (1979) 559.
- 26 D. Bonchev, D. Kamenski and V. Kamenska, God. Vissh. Khim.-Tekhnol. Inst., Burgas, Bulgaria, 10 (1973) 437.
- 27 M. Ferrario and M.W. Evans, Chem. Phys., 72 (1982) 141, 147.
- 28 P. Grigolini, J. Stat. Phys., 27 (1982) 283.
- 29 P. Grigolini, Mol. Phys., 31 (1976) 1717.
- 30 M.W. Evans, P. Grigolini and F. Marchesoni, Phys. Rev. Letters, in prep.
- 31 M. Suzuki, Adv. Chem. Phys., 46 (1981) 195.